Published OnlineFirst March 7, 2017; DOI: 10.1158/1078-0432.CCR-16-2601

Biology of Human Tumors

Clinical Cancer Research

PD-L1 Is a Therapeutic Target of the Bromodomain Inhibitor JQ1 and, Combined with HLA Class I, a Promising Prognostic Biomarker in Neuroblastoma

Ombretta Melaiu[1], Marco Mina[2,3], Marco Chierici[2], Renata Boldrini[4], Giuseppe Jurman[2], Paolo Romania[1], Valerio D'Alicandro[1], Maria C. Benedetti[4], Aurora Castellano[5], Tao Liu[6], Cesare Furlanello[2], Franco Locatelli[5,7], and Doriana Fruci[1]

Abstract

Purpose: This study sought to evaluate the expression of programmed cell death-ligand-1 (PD-L1) and HLA class I on neuroblastoma cells and programmed cell death-1 (PD-1) and lymphocyte activation gene 3 (LAG3) on tumor-infiltrating lymphocytes to better define patient risk stratification and understand whether this tumor may benefit from therapies targeting immune checkpoint molecules.

Experimental Design: *In situ* IHC staining for PD-L1, HLA class I, PD-1, and LAG3 was assessed in 77 neuroblastoma specimens, previously characterized for tumor-infiltrating T-cell density and correlated with clinical outcome. Surface expression of PD-L1 was evaluated by flow cytometry and IHC in neuroblastoma cell lines and tumors genetically and/or pharmacologically inhibited for MYC and MYCN. A dataset of 477 human primary neuroblastomas from GEO and ArrayExpress databases was explored for PD-L1, MYC, and MYCN correlation.

Results: Multivariate Cox regression analysis demonstrated that the combination of PD-L1 and HLA class I tumor cell density is a prognostic biomarker for predicting overall survival in neuroblastoma patients ($P = 0.0448$). MYC and MYCN control the expression of PD-L1 in neuroblastoma cells both *in vitro* and *in vivo*. Consistently, abundance of PD-L1 transcript correlates with MYC expression in primary neuroblastoma.

Conclusions: The combination of PD-L1 and HLA class I represents a novel prognostic biomarker for neuroblastoma. Pharmacologic inhibition of MYCN and MYC may be exploited to target PD-L1 and restore an efficient antitumor immunity in high-risk neuroblastoma. *Clin Cancer Res; 23(15); 4462–72. ©2017 AACR.*

Introduction

The prognostic value of tumor-infiltrating immune cells has been extensively demonstrated in several human cancers (1). According to *in situ* IHC analysis, all types of immune cells can infiltrate tumors, either promoting or inhibiting their progression. In general, high density of effector and memory T cells has been correlated with good clinical outcome (2, 3), whereas the prevalence of myeloid cells is associated with poor prognosis (4).

Anticancer immunity can be impaired by a variety of immunosuppressive pathways, including the expression of inhibitory checkpoint receptors, such as programmed cell death-1 (PD-1), cytotoxic T lymphocyte–associated protein 4 (CTLA-4), and lymphocyte activation gene 3 (LAG3), which limit the effector function of T cells by interacting with their ligands expressed on a wide range of tumor cells (5–7). Blockade of PD-1 and programmed cell death-ligand-1 (PD-L1) by mAbs has provided encouraging results, especially in tumors characterized by high density of infiltrating T cells, detectable levels of PD-L1, and tumor-specific neoantigens (8–11). All these features have been shown to be predictive of a response to PD-1/PD-L1–blocking antibodies (10).

Despite the promising results on certain tumors in adults (11), little is known about the therapeutic potential of immune checkpoint inhibitors in neuroblastoma, the most common pediatric extracranial solid tumor, mainly occurring in children under the age of 5 years and accounting for 15% of childhood cancer-related death. Neuroblastoma displays the highest rate of spontaneous regression observed among human cancers, and one possible explanation for this phenomenon is the induction of patients' immune responses toward their own tumor cells (12). Consistent with this hypothesis, we have recently shown that tumor-infiltrating T cells have a prognostic value independent of the current criteria used for risk stratification of neuroblastoma (13). However, it is still unknown whether this antitumor immunity could benefit from treatment with immune checkpoint inhibitors. Few

[1]Immuno-Oncology Laboratory, Oncohaematology Department, Bambino Gesù Children's Hospital, IRCCS, Rome, Italy. [2]Fondazione Bruno Kessler, Trento, Italy. [3]Department of Computational Biology, University of Lausanne, Lausanne, Switzerland. [4]Pathology Department, Bambino Gesù Children's Hospital, IRCCS, Rome, Italy. [5]Paediatric Haematology/Oncology Department, Bambino Gesù Children's Hospital, IRCCS, Rome, Italy. [6]Children's Cancer Institute Australia, Lowy Cancer Research Center, University of New South Wales, Randwich, New South Wales, Australia. [7]University of Pavia, Pavia, Italy.

Note: Supplementary data for this article are available at Clinical Cancer Research Online (http://clincancerres.aacrjournals.org/).

F. Locatelli and D. Fruci contributed equally to this article.

Corresponding Author: Doriana Fruci, Bambino Gesù Children's Hospital, IRCCS, Viale di San Paolo 15, Rome 00146, Italy. Phone: 3906-6859-2657; Fax: 3906-6859-2904; E-mail: doriana.fruci@opbg.net

doi: 10.1158/1078-0432.CCR-16-2601

Published OnlineFirst March 7, 2017; DOI: 10.1158/1078-0432.CCR-16-2601

Translational Relevance

The emergence of promising immunotherapeutic approaches based on immune checkpoint inhibitors in treatment of cancer, and the little information available on their efficacy on neuroblastoma, prompted us to investigate the expression of immune checkpoints PD-1, LAG3, programmed cell death-ligand-1 (PD-L1), and of HLA-I in this malignancy. According to the density of PD-L1$^+$ and HLA-I$^+$ tumor cells, we distinguish two combinations: one associated with good prognosis and another associated with poor prognosis. Multivariate Cox regression analysis revealed that PD-L1/HLA-I combination is a prognostic biomarker for predicting overall survival in neuroblastoma patients. In addition, we demonstrated that MYC and MYCN control PD-L1 expression in neuroblastoma and that they are targets of the bromodomain inhibitor JQ1. Taken together, our findings identify PD-L1/HLA-I combination as a novel prognostic biomarker for neuroblastoma and the pharmacologic inhibition of MYCN and MYC as a new therapeutic strategy to target PD-L1 and potentially restore an efficient antitumor immunity in high-risk neuroblastoma.

studies have investigated PD-L1 and PD-1 expression in neuroblastoma with discordant results. Some authors detected a high frequency of PD-L1$^+$ tumor cells (31/43 samples) in high-risk neuroblastoma (14), whereas others reported no expression of PD-L1 in 18 primary and 4 metastatic neuroblastoma lesions tested (15, 16). A detailed description of the functional status of tumor-infiltrating immune cells in a larger cohort of neuroblastoma samples is not currently available.

To address this issue, we studied the relationship between density of PD-L1$^+$ and HLA class I$^+$ (HLA-I) tumor cells, PD-1$^+$ and LAG3$^+$ tumor-infiltrating lymphocytes (TIL), and clinical outcome in 77 neuroblastoma samples. We defined two groups of patients based on PD-L1 and HLA-I tumor cell densities: a group in which PD-L1 is absent and the clinical outcome is driven by HLA-I, and a second group where the presence of PD-L1 directly affects the prognosis. Multivariate Cox regression analysis revealed that the combined PD-L1 and HLA-I tumor cell density predicts the clinical outcome in neuroblastoma patients. In addition, we found that both MYC and MYCN control PD-L1 expression in human neuroblastoma cell lines both *in vitro* and *in vivo*. Consistently, abundance of PD-L1 transcript correlated with MYC expression in 477 human primary neuroblastoma. Altogether, these findings open novel potential perspectives for the treatment of this aggressive pediatric malignancy.

Materials and Methods

Patients

Tumor samples from 77 neuroblastoma patients diagnosed between 2002 and 2015 at the Bambino Gesù Children's Hospital (Rome, Italy) were used. All tissues were obtained at diagnosis and prior to any therapy. Written informed parental consent was obtained for each patient in accordance with the Declaration of Helsinki. The study was approved by the Ethical Committee of the Institution. Clinical information is detailed in Supplementary Table S1. Diagnosis and histology were performed according to the International Neuroblastoma Staging System (INSS) and the International Neuroblastoma Pathology Classification (17, 18), respectively. MYCN and 1p status were evaluated following current guidelines (19). Patients were treated according to protocols active for different risk groups (20–23). Two high-risk patients were treated with anti-GD2 antibody and IL2 according to the HR-NBL-1/SIOPEN protocol (ClinicalTrials.gov Identifier: NCT01704716). Both patients are alive at 2 and 5 years from the diagnosis, respectively.

Antibodies, flow cytometry, and immunoblotting

The following antibodies were used: PD-L1 (RBT-PDL1, Bio SB), β2m-free HLA-I heavy chains (HC10; ref. 24), PD-1 (NAT105, ScyTek Laboratories), LAG3 (EPR4392(2), Abcam), and MYCN (TA351452, OriGene) for IHC; MYCN, actin (B8.4. B and I-19, respectively, Santa Cruz Biotechnology), and MYC (Y69, OriGene) for Western blotting; PD-L1 (MIH1, BD Biosciences) for flow cytometry. Apoptosis was detected by staining with APC-conjugated Annexin V and propidium iodide (BD Bioscences). Flow cytometry was performed on BD LSR Fortessa X20 with FACSDiva Software (BD Bioscences). Whole-cell extracts were obtained, quantified, and used as described previously (25).

IHC and acquisition

Formaldehyde-fixed paraffin-embedded blocks were cut into 4-μm sections and stored at 4°C until IHC evaluation was performed. Sections were baked for 60 minutes at 56°C in a dehydration oven, and antigen retrieval and deparaffinization were carried out on a PT-Link (Dako) using the EnVision FLEX Target Retrieval Solution Kits at high or low pH (Dako), as per the manufacturer's instructions. Following unmasking, slides were blocked for endogenous peroxidase for 10 minutes with a peroxidase blocking solution (Dako), rinsed in the appropriate wash buffer (Dako), and incubated for 30 minutes with 5% PBS/BSA. Slides were then incubated overnight at 4°C with primary antibodies. This step was followed by incubation with secondary antibody coupled with peroxidase (Dako) for 20 minutes. Bound peroxidase was detected with diaminobenzidine solution and EnVision FLEX Substrate buffer containing peroxide (Dako). Tissue sections were counterstained with EnVision FLEX hematoxylin (Dako). Sections of normal tonsils were used as positive controls (Supplementary Fig. S1A-D). Isotype-matched mouse mAbs were used as negative controls. Slides were analyzed using an image analysis workstation (D-SIGHT Menarini Diagnostic). The density of PD-L1$^+$ and HLA-I$^+$ tumor cells and tumor-infiltrating PD-1$^+$ and LAG3$^+$ lymphocytes was recorded by two blinded examiners as the number of positive cells per unit tissue surface area (mm^2). The mean of positive cells detected in 10 fields for each sample was used in the downstream statistical analysis. Each quantity x was converted to the log scale with the formula $y = ln\ (x + 1\ /\ (1 + x))$ to allow the transformation of any nonnegative value.

Cell lines, mice, and reagents

Human neuroblastoma cell lines were obtained in 2014 as follows: IMR-32, SK-N-BE(2), SH-EP, SH-SY5Y, SK-N-AS, and SK-N-SH from the ATCC, LA-N-1 from Creative Bioarray, KCNR from Children's Oncology Group Cell Culture, DSMZ, ACN, and GICAN from Interlab Cell Line Collection, Banca Biologica, and Cell Factory. Tet-21/N cell line was kindly provided by Dr M. Schwab (University of Tübingen, Tübingen, Germany). All cells were grown in RPMI1640 medium, last authenticated by HLA-I

Published OnlineFirst March 7, 2017; DOI: 10.1158/1078-0432.CCR-16-2601

typing (PCR-SSP, GenoVision), and last tested for mycoplasma contamination (VenorGem OneStep Kit, Minerva Biolabs) in mid-2016. For *in vivo* studies, animal experiments were conducted under the auspices of protocols approved by the Animal Care and Ethics Committee of the University of New South Wales (New South Wales, Australia). Tissue sections of SK-N-BE (2) xenografts from 5- to 6-week-old female Balb/c mice treated with control solvent or JQ1 (4 and 6 mice, respectively; ref. 26) were stained with MYCN and PD-L1 antibodies. JQ1 (Selleckchem) was dissolved in DMSO and used at concentrations of 1 μmol/L for LAN-1, SK-N-BE(2), and Tet-21/N and 1.5 μmol/L for SK-N-AS cells (26).

Lentiviral infection

Tumor cells were infected with lentiviral particles generated as described previously (27) with a nontarget shRNA control vector (SHC002) or MYC shRNA (clone ID: TRC0000039642; Sigma-Aldrich).

Gene expression analysis

Agilent microarray gene expression data of 477 neuroblastoma patients (392 MYCN nonamplified, 83 MYCN amplified, 2 not evaluated; refs. 28, 29) were quantile normalized using the limma R package and then corrected for batch effects by the ComBat R package before downstream analysis.

Statistical analysis

The Kaplan–Meier method was used for the estimation of overall survival (OS), relapse-free survival (RFS), and event-free survival (EFS) curves. The log-rank test, as implemented in the survival R package, was used to compare OS, RFS, and EFS between different groups of patients as described previously (13). Survival analysis was first performed in a univariate fashion, feature by feature. In the case of continuous variables (e.g., PD-L1, HLA-I), unless otherwise specified, the optimal threshold yielding the best dichotomic patient stratification was selected. The Siegmund–Miller minimal *P* value correction (30) was used to reduce type I errors, using 0.1 as high and low epsilon coefficients. For PD-1 and LAG3, patients were stratified according to the median of their distribution. For consistency and to avoid overfitting, in multivariate survival analysis, patients were stratified using, for each variable, the threshold selected in the respective univariate survival analysis. Student *t* test was used to compare density of T-cell subsets between INSS stages. Linear regression analysis was performed using the lm and rlm methods of the stats and MASS R libraries, respectively. Statistical analyses were performed in the R software environment. Variables reaching $P < 0.05$ in univariate analysis were included in Cox proportional hazards regression models using a backward stepwise selection. Results from the *in vitro* assays were statistically evaluated using a two-tailed Student *t* test.

Results

Density of PD-L1$^+$ tumor cells correlates with clinical outcome of neuroblastoma

To evaluate the biological and clinical significance of PD-L1 expression on neuroblastoma, we performed IHC analysis on a cohort of 77 neuroblastoma samples, previously characterized for type, density, and composition of tumor-infiltrating T cells (13). PD-L1 showed marked heterogeneity in neuroblastoma specimens with intense membrane staining associated with weak cytoplasmic staining (Fig. 1A). PD-L1 status was defined as positive when, on average, at least 1 tumor cell per mm^2 exhibited membrane staining. There were 51 specimens (66%) with none or, on average, less than 1 PD-L1$^+$ tumor cell per mm^2 and 26 samples with more than 1 PD-L1$^+$ tumor cell per mm^2. As shown in the PD-L1 density plot (Fig. 1B), deceased patients (red dots) fall into two groups, which either did or did not express PD-L1 (7 and 10 patients, respectively). Survival analysis for up to 14 years after primary resection was performed by stratifying the subjects according to the optimal cut-off value for PD-L1 density selected with the minimum *P* value approach. No significant correlation was detected for OS, RFS, and EFS (log-rank *P* values: 0.501, 0.188, and 0.616, respectively, Fig. 1C; Supplementary Fig. S1E and S1F).

Next, we determined whether PD-L1$^+$ tumor cell density was associated with the clinical outcome of neuroblastoma patients stratified according to the INSS. The distribution of PD-L1$^+$ tumor cells was statistically different between INSS stages, with lower PD-L1 density correlating with a favorable prognosis (Fig. 1D). Of note, stages III and IV included patients with either very high or very low PD-L1$^+$ tumor cell density (Fig. 1D).

Density of PD-L1$^+$ and HLA-I$^+$ tumor cells correlates with clinical outcome

High-risk neuroblastomas are associated with low HLA-I expression (31). As reduced HLA-I expression, by impairing cytotoxic T-cell function, yields a functional effect similar to that of PD-L1 overexpression, HLA-I expression was investigated by IHC in the same cohort of patients and correlated with PD-L1 tumor cell density. HLA-I showed heterogeneous or undetectable membrane staining in tumor cells (Fig. 1A). HLA-I status was defined as positive when, on average, more than 5% of tumor cells exhibited membrane staining. Twenty-nine specimens (40%) were HLA-I negative, and most of deceased patients (red dots) belong to this group (Fig. 1B). Survival analysis performed by stratifying the subjects according to the cut-off value of 5% for HLA-I$^+$ tumor cells selected with the minimum *P* value approach revealed significant correlation with patient outcome. Specifically, HLA-I$^+$ tumor cell density supported the stratification of patients into groups with different OS, RFS, and EFS (log-rank *P* values: 5.22×10^{-6}, 7.34×10^{-3}, and 7.1×10^{-5}, respectively, Fig. 1C; Supplementary Fig. S1E and S1F). When patients were stratified according to the INSS, the distribution of HLA-I$^+$ tumor cells was statistically different between INSS stages, with a higher HLA-I$^+$ tumor cell density associated with less aggressive stages (Fig. 1D).

Interestingly, density of HLA-I$^+$ tumor cells was inversely correlated with PD-L1 ($r^2 = 0.073$, $P = 0.04$; Fig. 1E, gray line). This inverse correlation was even stronger when only PD-L1$^+$ tumor samples were considered ($r^2 = 0.196$, $P = 0.038$; Fig. 1E, red line). Of note, deceased patients (red plots) express less than 5% of HLA-I and either high or no PD-L1.

The complex relationship between PD-L1/HLA-I expression and clinical outcome prompted us to speculate about the existence of two populations in which PD-L1 and HLA-I play different roles: a first group of patients in which PD-L1 is absent and the clinical outcome is completely driven by HLA-I, and a second group where the presence of PD-L1 directly affects prognosis. To test this hypothesis, the contribution of the combined effect of PD-L1 and HLA-I was investigated. Patients were stratified according to PD-L1$^+$ and HLA-I$^+$ tumor cell densities. In the absence of PD-L1$^+$ tumor cells (PD-L1^{No}), density of HLA-I was significantly

Published OnlineFirst March 7, 2017; DOI: 10.1158/1078-0432.CCR-16-2601

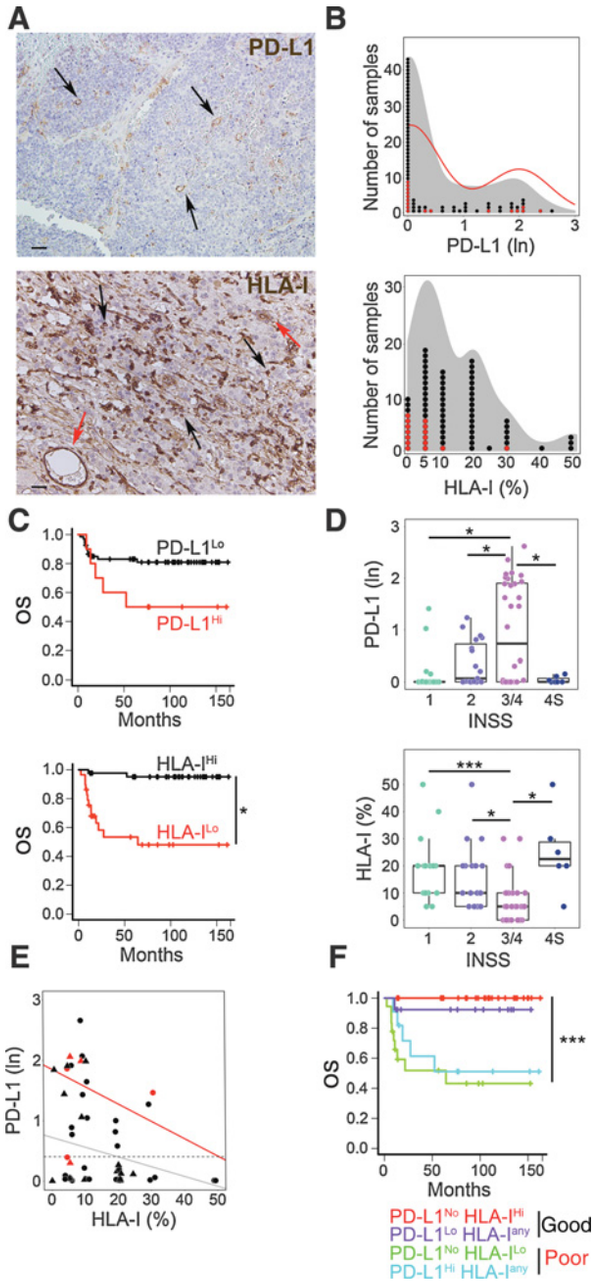

Figure 1.

PD-L1$^+$ and HLA-I$^+$ tumor cell densities are associated with clinical outcome in neuroblastoma. **A,** Representative examples of PD-L1$^+$ and HLA-I$^+$ cell staining in primary neuroblastoma lesions. Brown, PD-L1$^+$ and HLA-I$^+$ cells. Nuclei are counterstained with hematoxylin (blue). Black arrows, PD-L1$^+$ and HLA-I$^+$ tumor cells; red arrows, HLA-I$^+$ endothelial cells. Original magnification, ×20. Scale bar, 30 μm. **B,** Density plot of PD-L1$^+$ and HLA-I$^+$ tumor cells in neuroblastoma samples. Black and red dots, children who are alive and dead, respectively; gray plot, density of PD-L1$^+$ or HLA-I$^+$ tumor cells in all patients; red line, density of PD-L1$^+$ tumor cells in dead patients. **C,** Kaplan–Meier curves show the duration of OS according to the PD-L1$^+$ or HLA-I$^+$ tumor cell densities. High (Hi) and low (Lo) PD-L1$^+$ and HLA-I$^+$ cell densities were plotted according to the cut-off values that yielded the minimum *P* values for OS. **D,** Box plots of the PD-L1$^+$ and HLA-I$^+$ tumor cell densities according to the INSS stages. The boxes show the 25th to 75th percentile; the horizontal lines inside the box represent the median; the whiskers extend to the most extreme data point, which is no more than 1.5 times the interquartile range from the box; and the dots are individual samples. **E,** Scatter plot showing the correlation between PD-L1$^+$ and HLA-I$^+$ tumor cell densities. Dashed horizontal line, PD-L1 threshold 0.406 for PD-L1–expressing patients; black and red dots, alive and dead patients, respectively; triangles and dots, MYCN-amplified and nonamplified patients, respectively; red and gray lines, best-fit linear lines of the scatter plot for PD-L1–expressing patients and all patients, respectively. **F,** Kaplan–Meier curves of OS according to the combined PD-L1$^+$ and HLA-I$^+$ tumor cell densities. *, $P < 0.05$; ***, $P < 0.0001$.

associated with prognosis, for example, high and low amount of HLA-I$^+$ tumor cells (defined as samples with more and less than 5% of HLA-I$^+$ tumor cell density, respectively) correlated with good and poor prognosis, respectively (log-rank *P* values for OS, RFS, and EFS: 8.8×10^{-6}, 1.58×10^{-2}, and 4.6×10^{-4}, respectively, Fig. 1F; Supplementary Fig. S1G and S1H). Conversely, HLA-I tumor cell density appeared not to influence the outcome of PD-L1–expressing patients. Specifically, high and low PD-L1$^+$ tumor cell density (defined as samples with more than 5 and between 1 and 5 PD-L1$^+$ tumor cells, respectively, Supplementary Fig. S1I) correlated with poor and good prognosis, respectively, in both cases regardless of HLA-I$^+$ tumor cell density (Fig. 1F). Thus, we can distinguish two PD-L1/HLA-I combinations, one associated with good prognosis and the other associated with poor prognosis.

A favorable PD-L1/HLA-I combination correlates with better clinical outcome regardless of tumor-infiltrating T-cell density, MYCN amplification, INSS stage, and age

Next, we investigated whether PD-L1 and HLA-I tumor cell densities could improve the prediction of clinical outcome of patients when combined with variables known to affect patient survival, such as the abundance of tumor-infiltrating T cells (13), MYCN amplification, INSS stage, and age at diagnosis.

Survival analysis was performed by stratifying patients according to density of tumor-infiltrating T cells alone (log-rank *P* values for OS: 4.54×10^{-4}, 4.35×10^{-3}, and 0.583 for CD3$^+$, CD4$^+$, and CD8$^+$ T cells, respectively), or in combination with PD-L1 and/or HLA-I (Fig. 2; Supplementary Fig. S2). High density of CD3$^+$ T cells was associated with good prognosis regardless of PD-L1$^+$ tumor cell density, whereas low density of CD3$^+$ T cells was associated with worse prognosis, in particular in patients with high PD-L1$^+$ tumor cell density (log-rank *P* values for OS: 0.01; Fig. 2B). Conversely, high density of HLA-I$^+$ tumor cells was associated with better clinical outcome in patients with either high or low tumor-infiltrating CD3$^+$ T cells (log-rank *P* value for OS: 7.3×10^{-5}, Fig. 2C). Similarly, the good PD-L1/HLA-I combination was associated with better prognosis regardless of tumor-infiltrating CD3$^+$ T-cell density (log-rank *P* values for OS: 4.9×10^{-5}, Fig. 2D). Similar results were observed with tumor-infiltrating CD4$^+$ T-cell density (log-rank *P* values for OS: 0.01, 1×10^{4}, and 8.5×10^{-5}, with PD-L1, HLA-I, and PD-L1/HLA-I combination, respectively, Supplementary Fig. S2B–S2D). Conversely, high density of CD8$^+$ T cells did not improve patient stratification when combined with PD-L1 (log-rank *P* value for OS: 0.433), whereas it was associated with better prognosis when combined with high HLA-I or good PD-L1/HLA-I, and worse prognosis when combined with low HLA-I or poor PD-L1/HLA-I (log-rank *P* values for OS: 2.7×10^{-6} and 1.03×10^{-8},

Published OnlineFirst March 7, 2017; DOI: 10.1158/1078-0432.CCR-16-2601

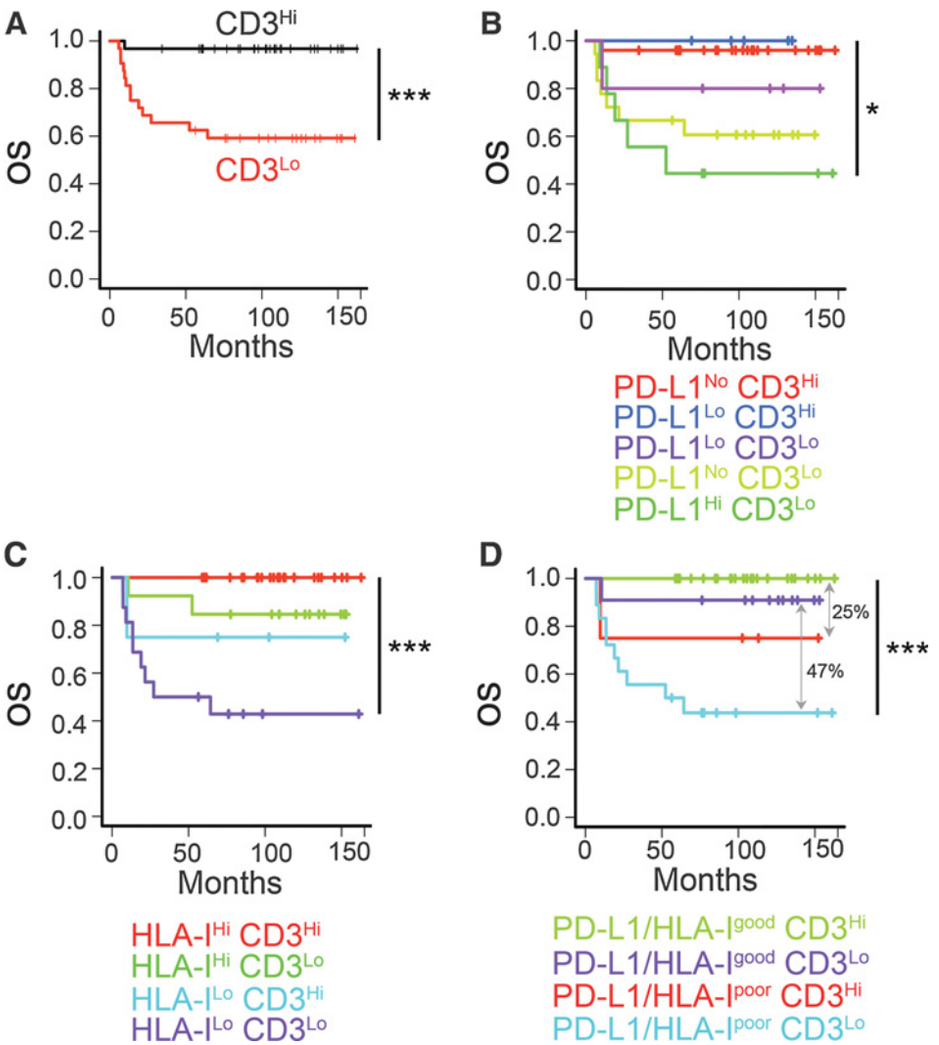

Figure 2.
Favorable PD-L1/HLA-I combination associates with better clinical outcome in neuroblastoma regardless of the density of tumor-infiltrating T cells. **A–D,** Kaplan–Meier curves of OS according to the density of tumor infiltrating $CD3^+$ T cells alone (**A**) or combined with PD-$L1^+$ tumor cell density (**B**), HLA-I^+ tumor cell density (**C**), or both (**D**). Gray arrows, increased OS between the selected groups. *, $P < 0.05$; ***, $P < 0.0001$.

respectively, Supplementary Fig. S2F–S2H). Significant *P* values were also observed for PD-L1/HLA-I combined with density of infiltrating $CD3^+$, $CD4^+$, and $CD8^+$ T-cell subsets for predicting RFS and EFS (log-rank *P* values: 5.4×10^{-3}, 9.8×10^{-3}, and 6.6×10^{-5}, respectively for RFS, and 2.04×10^{-3}, 3.94×10^{-3}, and 1.27×10^{-6}, respectively for EFS, Supplementary Fig. S3).

Density of PD-1^+ and $LAG3^+$ infiltrating lymphocytes was evaluated in the same cohort of patients by IHC analysis (Fig. 3A) and correlated with PD-$L1^+$ and/or HLA-I^+ tumor cell densities. The number of PD-1^+ and $LAG3^+$ infiltrating lymphocytes was proportional to the density of TILs (*P* values: 2×10^{-16} and 2×10^{-16} for PD-1 and LAG3, respectively) and lymphoid aggregates (Fig. 3B; Supplementary Fig. S4A). On average, 16% of TILs expressed PD-1, whereas 24% expressed LAG3. Survival analysis performed by stratifying patients according to the median cut-off values of PD-1^+ and $LAG3^+$ lymphocyte densities did not significantly correlate with patient outcome (log-rank *P* values: 0.1.7 and 6.7×10^{-2}, respectively, Supplementary Fig. S4B). The distribution of PD-1^+ lymphocytes was statistically different between INSS stages (Fig. 3C). Of note, density of PD-1^+ lymphocytes was inversely correlated with PD-$L1^+$ tumor cell density ($r^2 = 0.389$, $P = 0.0017$, Fig. 3D, red line).

High density of PD-1^+ and $LAG3^+$ infiltrating lymphocytes did not improve patient stratification when combined with PD-$L1^+$ (log-rank *P* values: 0.2 and 0.19, respectively), or HLA-I^+ tumor cell densities (log-rank *P* values: 1.06×10^{-4} and 9.6×10^{-5}, respectively; Supplementary Fig. S4C and S4D). Conversely, the good PD-L1/HLA-I combination was associated with better OS, RFS, and EFS regardless of PD-1^+ and $LAG3^+$ lymphocyte densities (log-rank *P* values: 5.3×10^{-6} and 9.8×10^{-6} for OS, 3.34×10^{-2} and 2.66×10^{-2} for RFS, and 1.21×10^{-3} and 8.36×10^{-4} for EFS, respectively, Fig. 3E; Supplementary Fig. S4E–S4H).

To determine whether favorable PD-L1/HLA-I combination was associated with better prognosis of MYCN-amplified neuroblastoma patients, survival analysis was performed by stratifying patients according to the MYCN status alone (log-rank *P* value: 1.1×10^{-4}, Fig. 4A), or in combination with PD-L1 and/or HLA-I. Density of PD-$L1^+$ or HLA-I^+ tumor cells affects prognosis of both MYCN-amplified and nonamplified neuroblastoma patients (log-rank *P* values for OS: 1.68×10^{-3} and 4.47×10^{-8}, respectively, Supplementary Fig. S5A and S5B). Specifically, the absence or low PD-$L1^+$ and high HLA-I^+ tumor cell densities were associated with better survival of both MYCN-amplified and nonamplified neuroblastoma patients.

Published OnlineFirst March 7, 2017; DOI: 10.1158/1078-0432.CCR-16-2601

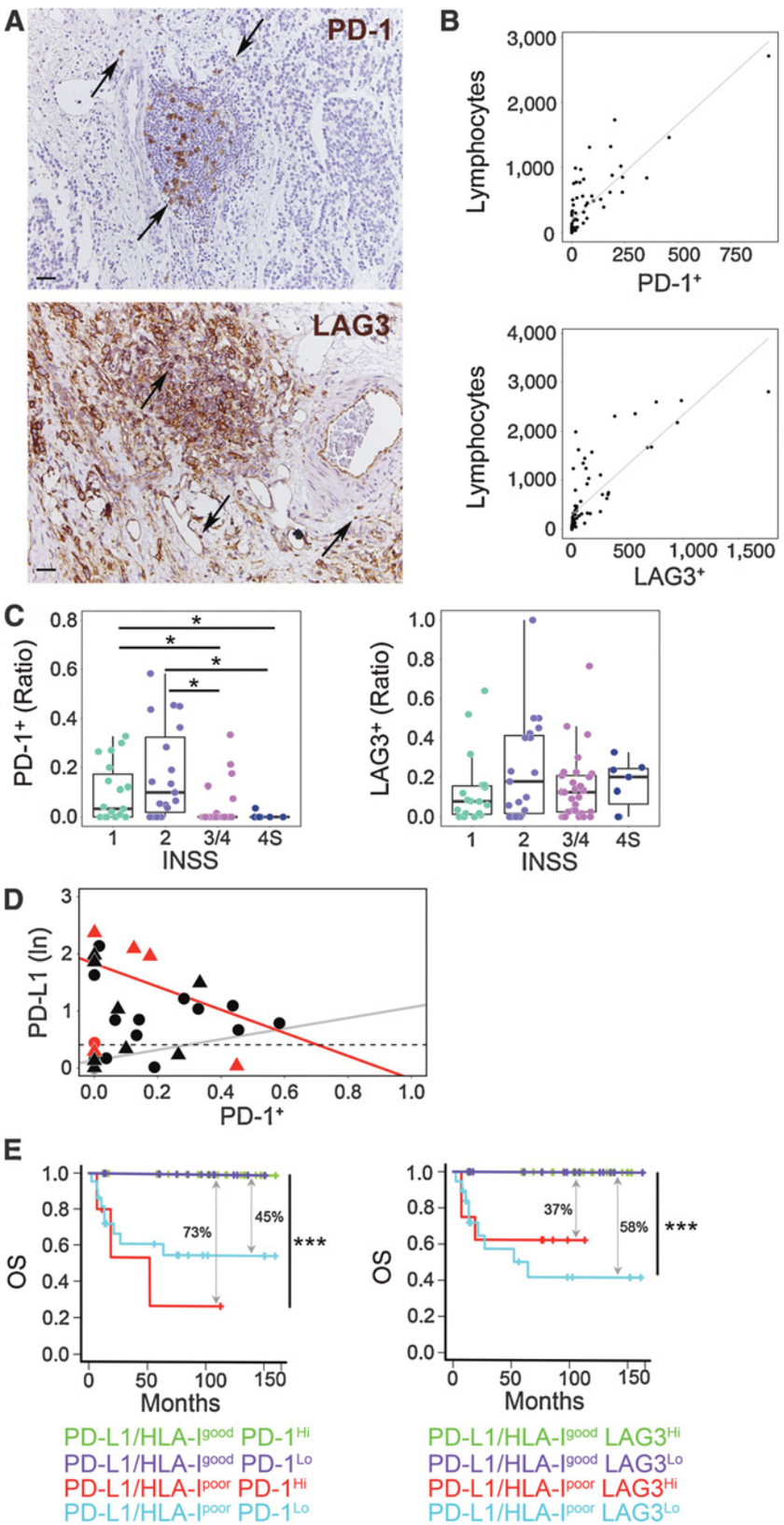

Figure 3.

Favorable PD-L1/HLA-I combination associates with better clinical outcome in neuroblastoma regardless of tumor-infiltrating PD-1$^+$ and LAG3$^+$ lymphocyte densities. **A,** Representative examples of PD-1$^+$ and LAG3$^+$ cell staining in primary neuroblastoma lesions. Brown, PD-1 and LAG3-expressing lymphocytes. Nuclei are counterstained with hematoxylin (blue). Black arrows, PD-1$^+$ and LAG3$^+$ lymphocytes localized in lymphoid aggregates or scattered in the neuroblastoma tissue. Original magnification, ×20. Scale bar, 30 μm. **B,** Scatter plots showing the correlation between the total number of lymphocytes and PD-1$^+$ or LAG3$^+$ lymphocytes. **C,** Box plots of the PD-1$^+$ and LAG3$^+$ lymphocyte densities according to the INSS stages. **D,** Scatter plot showing the correlation between density of PD-1$^+$ infiltrating lymphocytes and PD-L1$^+$ tumor cells. Dashed line, PD-L1 threshold of 0.406; red and gray lines, best-fit linear lines of the scatter plot for PD-L1–expressing patients and all patients, respectively. **E,** Kaplan–Meier curves of OS of patients according to the combined density of PD-L1$^+$ and HLA-I$^+$ tumor cells with PD-1$^+$ or LAG3$^+$ infiltrating lymphocytes. Gray arrows, increased OS between the selected groups. *, $P < 0.05$; ***, $P < 0.0001$.

Published OnlineFirst March 7, 2017; DOI: 10.1158/1078-0432.CCR-16-2601

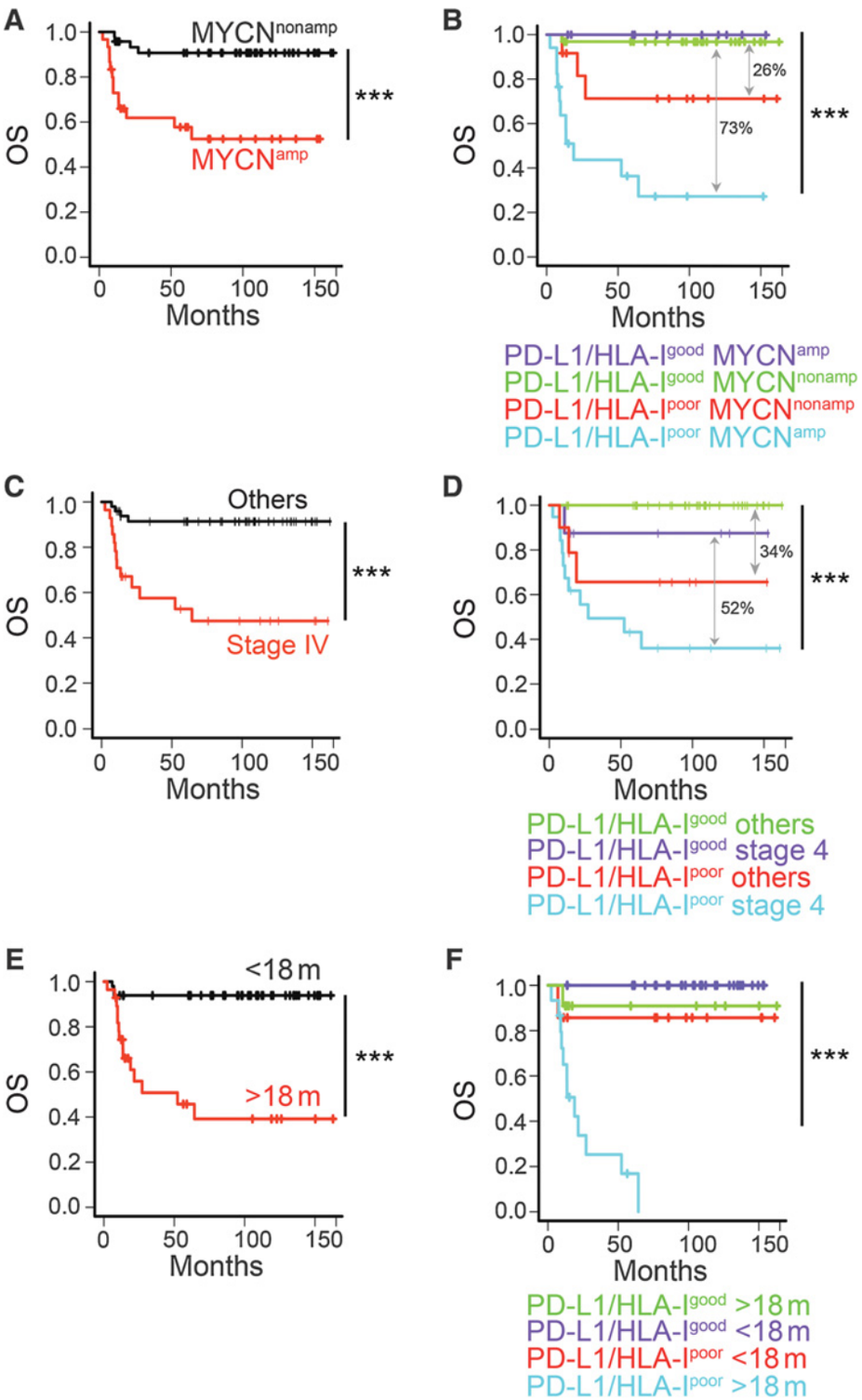

Figure 4.

Favorable PD-L1/HLA-I combination associates with better clinical outcome in neuroblastoma regardless of MYCN amplification, stage, and age at diagnosis. **A–F,** Kaplan–Meier curves of OS according to the MYCN amplification status alone (**A**) or combined with PD-L1$^+$ and HLA-I$^+$ tumor cell densities (**B**), the INSS groups (stage I–III and IVS vs. stage IV) alone (**C**) or combined with PD-L1$^+$ and HLA-I$^+$ tumor cell densities (**D**), and the age at diagnosis alone (**E**) or combined with PD-L1$^+$ and HLA-I$^+$ tumor cell densities (**F**). Gray arrows, increased OS between the selected groups. ***, $P < 0.0001$.

Accordingly, a good PD-L1/HLA-I combination correlated with better clinical outcome (log-rank P value: 2×10^{-8}, Fig. 4D). The presence of a "good" PD-L1/HLA-I combination was associated with a better survival of both nonamplified and MYCN-amplified neuroblastoma patients (26% and 73%, respectively).

Survival analysis performed by stratifying patients according to the INSS stage alone (log-rank P value: 3.2×10^{-5}, Fig. 4C), or in combination with PD-L1 and/or HLA-I, revealed that density of PD-L1$^+$ tumor cells did not improve patient stratification when combined with INSS stage (log-rank P value: 3.6×10^{-6},

Published OnlineFirst March 7, 2017; DOI: 10.1158/1078-0432.CCR-16-2601

Supplementary Fig. S5C). Conversely, high density of HLA-I$^+$ tumor cells and the good PD-L1/HLA-I combination were always associated with better prognosis (log-rank *P* values: 3.8×10^{-6} and 1.7×10^{-6}, respectively, Supplementary Fig. S5D; Fig. 4B). The presence of a "good" PD-L1/HLA-I combination was associated with a better survival of neuroblastoma patients with both favorable (stages I–III and IVS) and unfavorable (stage IV) prognosis (34% and 52%, respectively, Fig. 4D).

Survival analysis performed by stratifying patients according to the age cutoff of 18 months at diagnosis alone (log-rank *P* value: 1.76×10^{-6}, Fig. 4E), or in combination with PD-L1 and/or HLA-I, revealed that age <18 months was associated with better survival regardless of the density of PD-L1$^+$ (log-rank *P* value: 3.56×10^{-5}, Supplementary Fig. S5E). High density of HLA-I$^+$ tumor cells or the good PD-L1/HLA-I combination was associated with better prognosis (log-rank *P* values: 1.3×10^{-10} and 2.84×10^{-12}, respectively, Supplementary Fig. S5F; Fig. 4F). Similar results were obtained using a 365-day age cutoff (not shown). Significant *P* values were also observed for PD-L1/HLA-I versus MYCN, stage, or age for predicting RFS and EFS (log-rank *P* values: 4.2×10^{-4}, 2.11×10^{-6}, and 9.43×10^{-8} for RFS, and 7.24×10^{-6}, 8.4×10^{-5}, and 9.93×10^{-10} for EFS, respectively, Supplementary Fig. S6).

To dissect the relative contribution of all variables known to favorably influence patient survival in univariate analysis (namely, INSS stage I–III and IVS, absence of MYCN amplification, high T-cell infiltration, age <18 months, and good PD-L1/HLA-I combination), a multivariate Cox regression analysis was performed. Only a favorable PD-L1/HLA-I combination remained statistically associated with better survival (HR, 0.0921; 95% confidence interval, 0.0089–0.9467; $P = 4.48 \times 10^{-2}$). These results demonstrate that the combination of PD-L1 and HLA-I represents a novel prognostic variable for predicting overall survival in neuroblastoma patients.

MYC and MYCN regulate PD-L1 expression in neuroblastoma

The extremely variable expression of PD-L1 in stages III and IV neuroblastoma patients (Fig. 1D) suggests the existence of a complex mechanism of regulation. Recently, the *MYC* oncogene has been shown to induce PD-L1 expression in primary human samples of T-cell acute lymphoblastic leukemia (T-ALL; ref. 32). As MYC and MYCN share some transcriptional targets, we hypothesized that they both could regulate PD-L1 expression in neuroblastoma. To test this hypothesis, PD-L1 cell surface expression was evaluated in a panel of 10 human neuroblastoma cell lines expressing different levels of MYC and MYCN proteins (Fig. 5A and B). PD-L1 was expressed at high levels in three neuroblastoma cell lines (GICAN, SH-EP, and SK-N-AS) and at low levels in all other cell lines (Fig. 5B; Supplementary Fig. S7A).

Next, the effect of genetic and/or pharmacologic inhibition of MYC and MYCN on PD-L1 expression was investigated in SK-N-AS, LAN-1, and SK-N-BE(2) cell lines, which are mutually exclusive for MYC or MYCN expression, and in the neuroblastoma cell line SH-EP–derived Tet-21/N carrying a tetracycline-repressible MYCN transgene. MYC suppression by shRNA (shMYC) or JQ1 treatment significantly reduced PD-L1 surface expression in SK-N-AS and Tet21/N, as compared with control shRNA-transduced cells (shCTRL) and untreated cells (Fig. 5C and D; Supplementary Fig. S7B). Of note, JQ1 treatment did not induce apoptosis as evaluated by Annexin V (Supplementary Fig. S7C). Interestingly, PD-L1 surface expression was also significantly reduced in JQ1-treated LAN-1 and SK-N-BE(2) cells following MYCN protein reduction (Fig. 5E; Supplementary Fig. S7B). Consistent with these observations, suppression of MYCN by JQ1 resulted in a significant reduction of PD-L1 protein expression in SK-N-BE(2) xenografts (Fig. 5F), suggesting that both transcription factors regulate PD-L1 expression in neuroblastoma cells.

Finally, we explored a dataset of 477 human primary neuroblastomas from the FDA SEQC initiative publicly available in GEO and ArrayExpress databases (28, 29). Consistently with *in vitro* data, PD-L1 expression was significantly correlated with MYC expression (Fig. 6A), confirming what was observed in liver, renal, and colon carcinomas (32). An inverse correlation was detected between PD-L1 and MYCN and between MYCN and MYC, with MYCN-amplified samples (dark gray dots) expressing lower levels of both PD-L1 and MYC (Fig. 6B and C). Of note, no correlation was detected between MYCN and PD-L1 when only MYCN nonamplified samples were analyzed ($r^2 = 0.006$, $P = 0.12$), suggesting that other genes coamplified in the same region may exert an inhibitory effect.

Altogether, these data indicate that MYC and MYCN control the expression of PD-L1 in neuroblastoma and that therapies suppressing the function of both these transcription factors may be exploited to restore an immune response against this tumor.

Discussion

Recently, we showed that high T-cell infiltration correlates with favorable clinical outcome in high-risk neuroblastoma patients (13). Herein, we demonstrate that TILs express PD-1 and LAG3, two negative regulators of T-cell function (33), and that neuroblastoma cells either express PD-L1 or HLA-I. According to the density of PD-L1$^+$ and HLA-I$^+$ tumor cells and regardless of infiltrating T-cell density, MYCN amplification status, INSS stage, and age at diagnosis, we could distinguish two PD-L1/HLA-I combinations: one associated with good prognosis (high HLA-I and low or no PD-L1) and the other associated with poor prognosis (low HLA-I and high or no PD-L1). Our findings provide a proof of principle that PD-L1 in combination with HLA-I expression may serve as a biomarker in neuroblastoma, although this has to be further confirmed by a prospective study with a larger number of samples.

Of note, a good PD-L1/HLA-I combination was also associated with favorable clinical outcome in intrahepatic cholangiocarcinoma and hepatocellular carcinoma (34, 35). Consistently, clinical trials with drugs targeting the PD-1/PD-L1 pathway have demonstrated that PD-L1 tumor density alone, initially chosen as a criterion for enrolling patients, did not prove to be a reliable biomarker, because of its variable expression in response to changes in the inflammatory microenvironment (33, 36, 37).

Interestingly, we found that the density of PD-1$^+$ and LAG3$^+$ lymphocytes was proportional to that of tumor-infiltrating immune cells and mainly distributed in lymphoid aggregates, structures that resemble lymph nodes (38). Tumor-infiltrating T cells are reactive against immunogenic tumor cells, namely tumor cells that display on their surface HLA-I molecules loaded with antigens derived either from proteins normally expressed in other tissues, or originated from point mutations in normal genes (8). According to a recent tumor genome meta-analysis, the amount

Published OnlineFirst March 7, 2017; DOI: 10.1158/1078-0432.CCR-16-2601

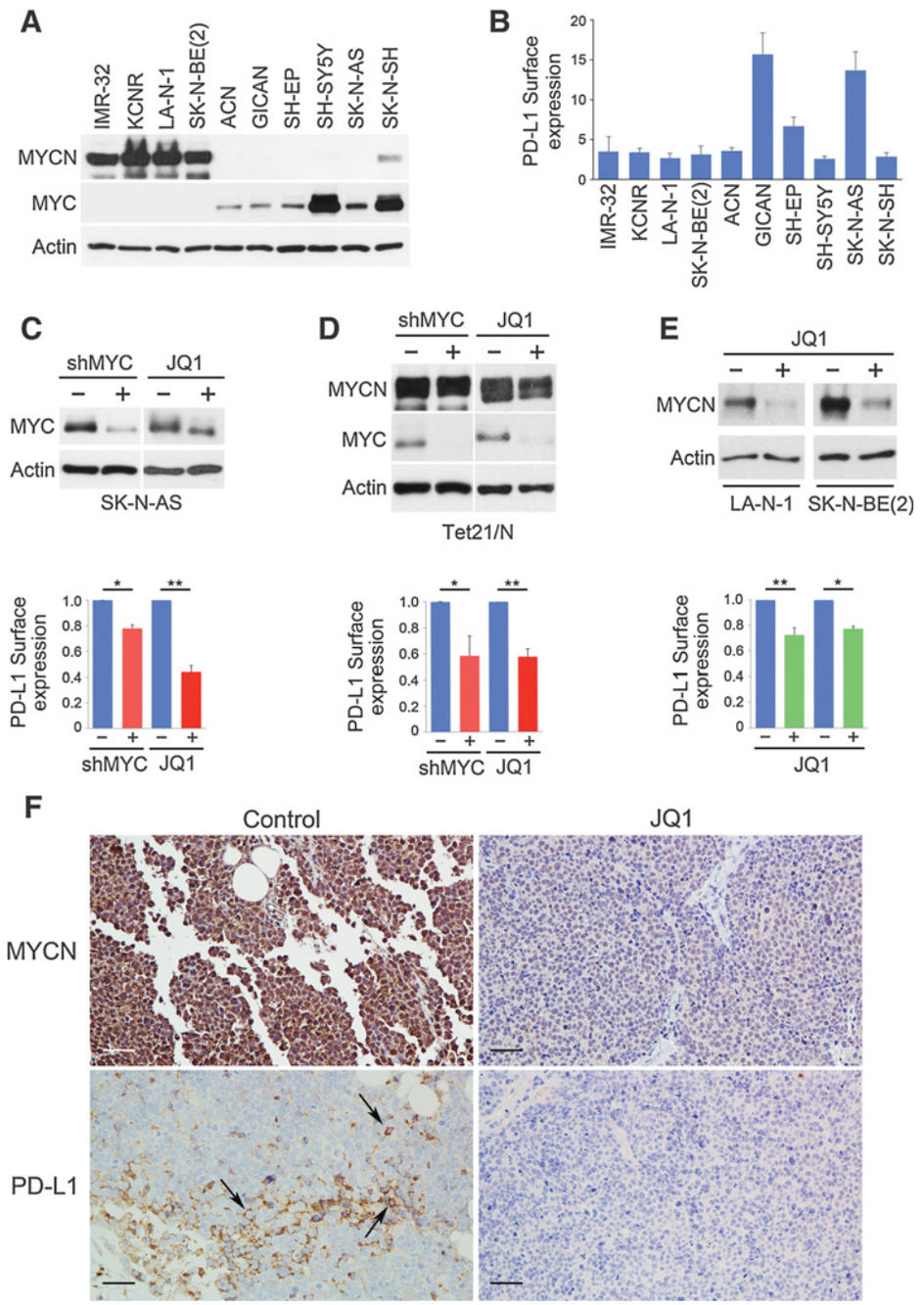

Figure 5.
MYC and MYCN regulate PD-L1 expression in neuroblastoma cells. **A,** Immunoblotting analysis of MYC and MYCN in neuroblastoma cell lines. An anti-actin Ab was used for normalization. **B,** Flow cytometry analysis of PD-L1 cell surface expression in neuroblastoma cell lines (mean ± SD, $n = 3$ biological replicates). **C,** Immunoblotting analysis of MYC and flow cytometry analysis of PD-L1 surface expression in SK-N-AS cells following MYC inhibition by shRNA or 72-hour JQ1 treatment (mean ± SD, $n = 4$ biological replicates). **D,** Immunoblotting analysis of MYC and MYCN and flow cytometry analysis of surface expression of PD-L1 in Tet21/N cells following MYC inhibition by shRNA or 72-hour JQ1-treatment (mean ± SD, $n = 4$ biological replicates). **E,** Immunoblotting analysis of MYCN and flow cytometry analysis of PD-L1 surface expression in the MYCN-amplified LA-N-1 and SK-N-BE(2) cells following MYCN inhibition by JQ1 treatment, for 48 and 72 hours, respectively (mean ± SD, $n = 4$ biological replicates). **F,** Representative examples of $MYCN^+$ and $PD\text{-}L1^+$ staining on SK-N-BE(2) tumors grown in nude mice treated intraperitoneally with control solvent (control) or JQ1 at 50 mg/kg body weight as described by Shahbazi and colleagues (26). Brown, MYCN and PD-L1–expressing cells. Nuclei are counterstained with hematoxylin (blue). Black arrows, $PD\text{-}L1^+$ tumor cells. Original magnification, ×20. Scale bar, 30 μm. *, $P < 0.05$; **, $P < 0.001$.

of mutations predicted to be immunogenic correlated with increased patient survival, higher T-cell infiltration, and the presence of neoantigens in proportion to the tumor mutational load (39). Although high-risk neuroblastomas harbor low genetic complexity, with significant mutations in only few genes, the intratumoral genetic heterogeneity due to germline variants and/or copy number alterations results in the expression of potentially immunogenic tumor antigens, such as MYCN, MYC, and ALK (40–42). Accordingly, $CD8^+$ T cells reactive toward MYCN, MYC, and ALK epitopes were detected in neuroblastoma, Burkitt lymphoma, and ALK-rearranged lymphoma patients, respectively, and were found to be associated with a decreased risk of relapse in some patients (43–47).

Although PD-L1 expression has been investigated in a wide range of tumors, the mechanism that controls its constitutive expression remained unclear. Several factors have been found to control PD-L1 expression (32, 48–50). Here, we report a new role for MYC and MYCN in regulating PD-L1 expression in neuroblastoma cells. Functional inhibition of MYC and/or MYCN by shRNA knockdown or JQ1 treatment resulted in a significant reduction of PD-L1 surface expression in neuroblastoma both *in vitro* and *in vivo*, thus suggesting that JQ1 (or related compounds

Published OnlineFirst March 7, 2017; DOI: 10.1158/1078-0432.CCR-16-2601

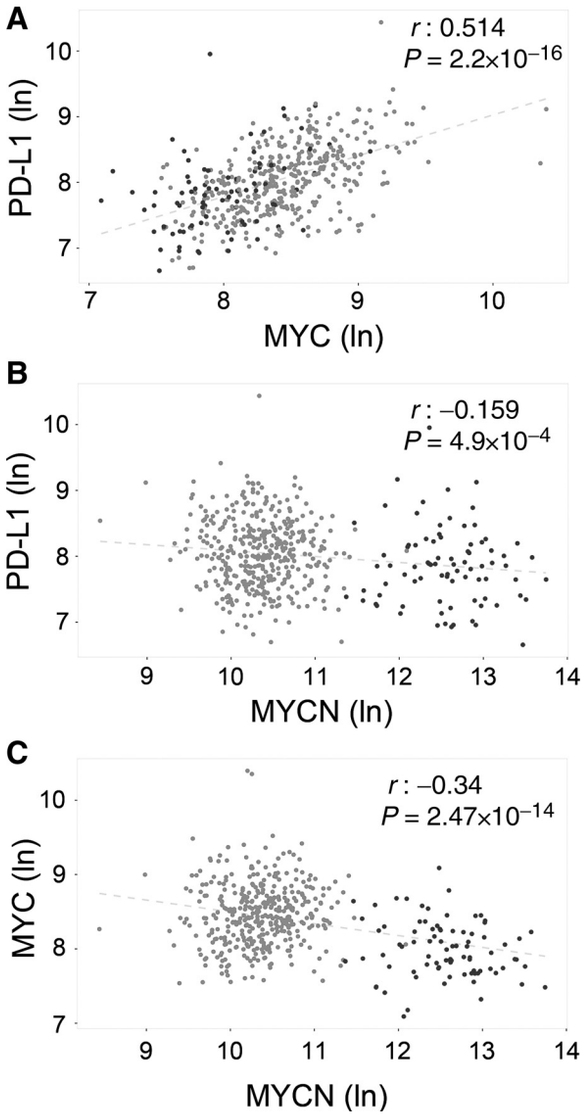

Figure 6.

Correlation of PD-L1, MYC, and MYCN expression in neuroblastoma specimens. **A–C,** Scatter plots showing the correlation between the expression of PD-L1 and MYC (**A**), PD-L1 and MYCN (**B**), and MYC and MYCN (**C**) in SEQC neuroblastoma patients. The best-fit linear lines and coefficients are shown. Dark and light gray dots, MYCN-amplified and nonamplified patients, respectively.

in clinical trials) might be well suited for neuroblastoma as both a targeted agent and an immunotherapeutic agent. Recently, Casey and colleagues showed that MYC regulates PD-L1 expression in human T-ALL samples through direct binding to its promoter (32). Consistently, we showed that MYC gene expression significantly correlated with PD-L1 transcript in a large cohort of neuroblastoma patients. In contrast, MYCN gene expression did not appear to correlate with PD-L1. We speculated that genes coamplified with MYCN could exert this inhibitory effect. Indeed, we found that most of the MYCN-amplified neuroblastoma cell lines and primary tissues lack PD-L1 expression.

In summary, our study demonstrates that (i) PD-L1 is expressed in neuroblastoma and is inversely correlated with HLA-I; (ii) the combination of PD-L1/HLA-I is a robust marker to predict clinical outcome; and (iii) MYC and MYCN regulate PD-L1 expression in neuroblastoma both *in vitro* and *in vivo*, indicating that their pharmacologic inhibition may represent a novel treatment strategy for targeting PD-L1 expression in high-risk neuroblastoma patients. In addition, these findings may be useful to predict neuroblastoma patients that will respond better to immunotherapy.

Disclosure of Potential Conflicts of Interest

No potential conflicts of interest were disclosed.

Authors' Contributions

Conception and design: O. Melaiu, F. Locatelli, D. Fruci
Development of methodology: O. Melaiu, M. Mina, P. Romania, V. D'Alicandro, M.C. Benedetti, D. Fruci
Acquisition of data (provided animals, acquired and managed patients, provided facilities, etc.): O. Melaiu, R. Boldrini, P. Romania, V. D'Alicandro, A. Castellano, T. Liu, D. Fruci
Analysis and interpretation of data (e.g., statistical analysis, biostatistics, computational analysis): O. Melaiu, M. Mina, M. Chierici, R. Boldrini, G. Jurman, C. Furlanello, D. Fruci
Writing, review, and/or revision of the manuscript: O. Melaiu, M. Chierici, G. Jurman, P. Romania, V. D'Alicandro, C. Furlanello, F. Locatelli, D. Fruci
Administrative, technical, or material support (i.e., reporting or organizing data, constructing databases): M. Mina, D. Fruci
Study supervision: F. Locatelli, D. Fruci

Acknowledgments

We thank P. Giacomini for providing reagents and M. Scarsella and M. Pezzullo for technical assistance.

Grant Support

This work was supported by Associazione Italiana per la Ricerca sul Cancro (AIRC, Milan, Italy) grants #18495 (to D. Fruci) and #9962 (to F. Locatelli), Italian Ministry of Health (Rome, Italy) grant PE-2011-02351866 (to D. Fruci), and Fondazione Italiana per la Lotta al Neuroblastoma (to F. Locatelli). This research was also supported by a fellowship from the Fondazione Umberto Veronesi (to O. Melaiu).

The costs of publication of this article were defrayed in part by the payment of page charges. This article must therefore be hereby marked *advertisement* in accordance with 18 U.S.C. Section 1734 solely to indicate this fact.

Received October 16, 2016; revised November 21, 2016; accepted March 1, 2017; published OnlineFirst March 7, 2017.

References

1. Fridman WH, Pages F, Sautes-Fridman C, Galon J. The immune contexture in human tumours: impact on clinical outcome. Nat Rev Cancer 2012; 12:298–306.
2. Galon J, Costes A, Sanchez-Cabo F, Kirilovsky A, Mlecnik B, Lagorce-Pages C, et al. Type, density, and location of immune cells within human colorectal tumors predict clinical outcome. Science 2006;313:1960–4.
3. Pages F, Berger A, Camus M, Sanchez-Cabo F, Costes A, Molidor R, et al. Effector memory T cells, early metastasis, and survival in colorectal cancer. N Engl J Med 2005;353:2654–66.
4. Bates GJ, Fox SB, Han C, Leek RD, Garcia JF, Harris AL, et al. Quantification of regulatory T cells enables the identification of high-risk breast cancer patients and those at risk of late relapse. J Clin Oncol 2006;24:5373–80.

5. Pardoll DM. The blockade of immune checkpoints in cancer immunotherapy. Nat Rev Cancer 2012;12:252–64.
6. Topalian SL, Drake CG, Pardoll DM. Immune checkpoint blockade: a common denominator approach to cancer therapy. Cancer Cell 2015; 27:450–61.
7. Zou W, Wolchok JD, Chen L. PD-L1 (B7-H1) and PD-1 pathway blockade for cancer therapy: mechanisms, response biomarkers, and combinations. Sci Transl Med 2016;8:328rv4.
8. Schumacher TN, Schreiber RD. Neoantigens in cancer immunotherapy. Science 2015;348:69–74.
9. Teng MW, Ngiow SF, Ribas A, Smyth MJ. Classifying Cancers Based on T-cell Infiltration and PD-L1. Cancer Res 2015;75:2139–45.
10. McGranahan N, Furness AJ, Rosenthal R, Ramskov S, Lyngaa R, Saini SK, et al. Clonal neoantigens elicit T cell immunoreactivity and sensitivity to immune checkpoint blockade. Science 2016;351:1463–9.
11. Mahoney KM, Rennert PD, Freeman GJ. Combination cancer immunotherapy and new immunomodulatory targets. Nat Rev Drug Discov 2015;14:561–84.
12. Bolande RP. A natural immune system in pregnancy serum lethal to human neuroblastoma cells: a possible mechanism of spontaneous regression. Perspect Pediatric Pathol 1992;16:120–33.
13. Mina M, Boldrini R, Citti A, Romania P, D'Alicandro V, De Ioris M, et al. Tumor-infiltrating T lymphocytes improve clinical outcome of therapy-resistant neuroblastoma. Oncoimmunology 2015;4:e1019981.
14. Chowdhury F, Dunn S, Mitchell S, Mellows T, Ashton-Key M, Gray JC. PD-L1 and CD8+PD1+ lymphocytes exist as targets in the pediatric tumor microenvironment for immunomodulatory therapy. Oncoimmunology 2015;4:e1029701.
15. Aoki T, Hino M, Koh K, Kyushiki M, Kishimoto H, Arakawa Y, et al. Low frequency of programmed death ligand 1 expression in pediatric cancers. Pediatr Blood Cancer 2016;63:1461–4.
16. Dondero A, Pastorino F, Della Chiesa M, Corrias MV, Morandi F, Pistoia V, et al. PD-L1 expression in metastatic neuroblastoma as an additional mechanism for limiting immune surveillance. Oncoimmunology 2016;5: e1064578.
17. Brodeur GM, Pritchard J, Berthold F, Carlsen NL, Castel V, Castelberry RP, et al. Revisions of the international criteria for neuroblastoma diagnosis, staging, and response to treatment. J Clin Oncol 1993;11:1466–77.
18. Shimada H, Ambros IM, Dehner LP, Hata J, Joshi VV, Roald B, et al. The international neuroblastoma pathology classification (the Shimada system). Cancer 1999;86:364–72.
19. Mathew P, Valentine MB, Bowman LC, Rowe ST, Nash MB, Valentine VA, et al. Detection of MYCN gene amplification in neuroblastoma by fluorescence in situ hybridization: a pediatric oncology group study. Neoplasia 2001;3:105–9.
20. Kohler JA, Rubie H, Castel V, Beiske K, Holmes K, Gambini C, et al. Treatment of children over the age of one year with unresectable localised neuroblastoma without MYCN amplification: results of the SIOPEN study. Eur J Cancer 2013;49:3671–9.
21. Rubie H, De Bernardi B, Gerrard M, Canete A, Ladenstein R, Couturier J, et al. Excellent outcome with reduced treatment in infants with nonmetastatic and unresectable neuroblastoma without MYCN amplification: results of the prospective INES 99.1. J Clin Oncol 2011;29:449–55.
22. De Bernardi B, Mosseri V, Rubie H, Castel V, Foot A, Ladenstein R, et al. Treatment of localised resectable neuroblastoma. Results of the LNESG1 study by the SIOP Europe Neuroblastoma Group. Br J Cancer 2008;99:1027–33.
23. De Ioris MA, Castellano A, Ilari I, Garganese MC, Natali G, Inserra A, et al. Short topotecan-based induction regimen in newly diagnosed high-risk neuroblastoma. Eur J Cancer 2011;47:572–8.
24. Stam NJ, Spits H, Ploegh HL. Monoclonal antibodies raised against denatured HLA-B locus heavy chains permit biochemical characterization of certain HLA-C locus products. J Immunol 1986;137:2299–306.
25. Lorenzi S, Forloni M, Cifaldi L, Antonucci C, Citti A, Boldrini R, et al. IRF1 and NF-kB restore MHC class I-restricted tumor antigen processing and presentation to cytotoxic T cells in aggressive neuroblastoma. PLoS One 2012;7:e46928.
26. Shahbazi J, Liu PY, Atmadibrata B, Bradner JE, Marshall GM, Lock RB, et al. The bromodomain inhibitor JQ1 and the histone deacetylase inhibitor panobinostat synergistically reduce N-Myc expression and induce anticancer effects. Clin Cancer Res 2016;22:2534–44.
27. Cifaldi L, Romania P, Falco M, Lorenzi S, Meazza R, Petrini S, et al. ERAP1 regulates natural killer cell function by controlling the engagement of inhibitory receptors. Cancer Res 2015;75:824–34.
28. Zhang W, Yu Y, Hertwig F, Thierry-Mieg J, Zhang W, Thierry-Mieg D, et al. Comparison of RNA-seq and microarray-based models for clinical endpoint prediction. Genome Biol 2015;16:133.
29. Oberthuer A, Juraeva D, Hero B, Volland R, Sterz C, Schmidt R, et al. Revised risk estimation and treatment stratification of low- and intermediate-risk neuroblastoma patients by integrating clinical and molecular prognostic markers. Clin Cancer Res 2015;21:1904–15.
30. Altman DG, Lausen B, Sauerbrei W, Schumacher M. Dangers of using "optimal" cutpoints in the evaluation of prognostic factors. J Natl Cancer Inst 1994;86:829–35.
31. Wolfl M, Jungbluth AA, Garrido F, Cabrera T, Meyen-Southard S, Spitz R, et al. Expression of MHC class I, MHC class II, and cancer germline antigens in neuroblastoma. Cancer Immunol Immunother 2005;54:400–6.
32. Casey SC, Tong L, Li Y, Do R, Walz S, Fitzgerald KN, et al. MYC regulates the antitumor immune response through CD47 and PD-L1. Science 2016;352:227–31.
33. Nguyen LT, Ohashi PS. Clinical blockade of PD1 and LAG3–potential mechanisms of action. Nat Rev Immunol 2015;15:45–56.
34. Sabbatino F, Villani V, Yearley JH, Deshpande V, Cai L, Konstantinidis IT, et al. PD-L1 and HLA Class I Antigen Expression and Clinical Course of the Disease in Intrahepatic Cholangiocarcinoma. Clin Cancer Res 2016;22:470–8.
35. Umemoto Y, Okano S, Matsumoto Y, Nakagawara H, Matono R, Yoshiya S, et al. Prognostic impact of programmed cell death 1 ligand 1 expression in human leukocyte antigen class I-positive hepatocellular carcinoma after curative hepatectomy. J Gastroenterol 2015;50:65–75.
36. Kinter AL, Godbout EJ, McNally JP, Sereti I, Roby GA, O'Shea MA, et al. The common gamma-chain cytokines IL-2, IL-7, IL-15, and IL-21 induce the expression of programmed death-1 and its ligands. J Immunol 2008; 181:6738–46.
37. Kryczek I, Wei S, Gong W, Shu X, Szeliga W, Vatan L, et al. Cutting edge: IFN-gamma enables APC to promote memory Th17 and abate Th1 cell development. J Immunol 2008;181:5842–6.
38. Gajewski TF, Schreiber H, Fu YX. Innate and adaptive immune cells in the tumor microenvironment. Nat Immunol 2013;14:1014–22.
39. Brown SD, Warren RL, Gibb EA, Martin SD, Spinelli JJ, Nelson BH, et al. Neo-antigens predicted by tumor genome meta-analysis correlate with increased patient survival. Genome Res 2014;24:743–50.
40. Sausen M, Leary RJ, Jones S, Wu J, Reynolds CP, Liu X, et al. Integrated genomic analyses identify ARID1A and ARID1B alterations in the childhood cancer neuroblastoma. Nat Genet 2013;45:12–7.
41. Pugh TJ, Morozova O, Attiyeh EF, Asgharzadeh S, Wei JS, Auclair D, et al. The genetic landscape of high-risk neuroblastoma. Nat Genet 2013;45: 279–84.
42. Cheung NK, Zhang J, Lu C, Parker M, Bahrami A, Tickoo SK, et al. Association of age at diagnosis and genetic mutations in patients with neuroblastoma. JAMA 2012;307:1062–71.
43. Himoudi N, Yan M, Papanastasiou A, Anderson J. MYCN as a target for cancer immunotherapy. Cancer Immunol Immunother 2008;57:693–700.
44. Sarkar AK, Nuchtern JG. Lysis of MYCN-amplified neuroblastoma cells by MYCN peptide-specific cytotoxic T lymphocytes. Cancer Res 2000; 60:1908–13.
45. Helm F, Kammertoens T, Lehmann FM, Wilke A, Bruns H, Mautner J, et al. Targeting c-MYC with T-cells. PloS One 2013;8:e77375.
46. Ait-Tahar K, Cerundolo V, Banham AH, Hatton C, Blanchard T, Kusec R, et al. B and CTL responses to the ALK protein in patients with ALK-positive ALCL. Int J Cancer 2006;118:688–95.
47. Passoni L, Gallo B, Biganzoli E, Stefanoni R, Massimino M, Di Nicola M, et al. *In vivo* T-cell immune response against anaplastic lymphoma kinase in patients with anaplastic large cell lymphomas. Haematologica 2006;91:48–55.
48. Chen J, Jiang CC, Jin L, Zhang XD. Regulation of PD-L1: a novel role of pro-survival signalling in cancer. Ann Oncol 2016;27:409–16.
49. Dorand RD, Nthale J, Myers JT, Barkauskas DS, Avril S, Chirieleison SM, et al. Cdk5 disruption attenuates tumor PD-L1 expression and promotes antitumor immunity. Science 2016;353:399–403.
50. Zhu H, Bengsch F, Svoronos N, Rutkowski MR, Bitler BG, Allegrezza MJ, et al. BET bromodomain inhibition promotes anti-tumor immunity by suppressing PD-L1 expression. Cell Rep 2016;16:2829–37.

AACR American Association for Cancer Research

Clinical Cancer Research

PD-L1 Is a Therapeutic Target of the Bromodomain Inhibitor JQ1 and, Combined with HLA Class I, a Promising Prognostic Biomarker in Neuroblastoma

Ombretta Melaiu, Marco Mina, Marco Chierici, et al.

Clin Cancer Res 2017;23:4462-4472. Published OnlineFirst March 7, 2017.